Journal of Peptide Science
J. Pept. Sci. 2007; **13**: 253–262
Published online in Wiley InterScience (www.interscience.wiley.com). DOI: 10.1002/psc.841

JOURNAL OF PEPTIDE SCIENCE

α,β-Dehydrophenylalanine containing cecropin–melittin hybrid peptides: conformation and activity

PUNITI MATHUR,[a] N. R. JAGANNATHAN[a] and V. S. CHAUHAN[b]*

[a] Department of N. M. R, All India Institute of Medical Sciences, New Delhi, India
[b] International Center for Genetic Engineering and Biotechnology, Aruna Asaf Ali Marg, New Delhi, India

Received 26 September 2006; Revised 28 December 2006; Accepted 10 January 2007

Abstract: Synthesis and conformational studies of a cecropin–melittin hybrid pentadecapeptide CA(1–7)MEL(2–9), and its three α, β-dehydrophenylalanine (ΔPhe) containing analogs in water-TFE mixtures are described. ΔPhe is placed at strategic positions in order to preserve the amphipathicity of the molecule. The wild type CAMEL0 and its three analogs, containing one, two and three ΔPhe residues namely CAMELΔPhe1, CAMELΔPhe2 and CAMELΔPhe3 respectively were synthesized in solid phase and their conformation determined by CD and NMR. CAMELΔPhe2 and CAMELΔPhe3 peptides exhibit the presence of 3_{10}-helix and β-turns in the former and only turns in the latter. CAMELΔPhe1 peptide was found to have a largely extended conformation. Antibacterial and hemolytic activities of the peptides were also evaluated. CAMELΔPhe2 peptide is maximally potent against both *Staphylococcus aureus* ATCC 259230 and *Escherichia coli* ATCC 11303. CAMELΔPhe1 with a single ΔPhe at the center shows minimal hemolysis. Copyright © 2007 European Peptide Society and John Wiley & Sons, Ltd.

Keywords: dehydroamino acids; bioactive peptides; cecropin; melittin; antibiotic peptides

INTRODUCTION

Antimicrobial peptides have been known to us for over two decades and are ubiquitous in nature as a part of the innate immune system and host defense mechanism [1–3]. They are produced by various species, both in prokaryotic and eukaryotic cells. Such peptides are constitutively expressed or induced by bacteria or their products. They are found in all species of life, ranging from viruses, bacteria, plants and insects to fish, molluscs, crustaceans, amphibians, birds, mammals and humans. These polycationic molecules possess highly diverse primary structures, yet their secondary structures share the common feature of amphipathicity. The peptides interact with the cell envelope membrane and then kill cells by a multihit mechanism that involves action on more than one anionic target. Ion channel or pore formation and the dissipation of the electrochemical gradient across the cell membrane are the main killing mechanisms for a majority of antimicrobial peptides. Some of the other potential intracellular targets include enzymes and nucleic acids [4–10]. These peptides are known to involve multiple targets and thus, can be highly effective. Topologically, antimicrobial peptides can be categorized into two: linear peptides and cysteine-bridged peptides. The first group can be further divided into two subgroups: (i) peptides adopting alpha-helical secondary structure and (ii) peptides of unusual composition, rich in Pro, Arg or Trp. Cysteine-bridged peptides can be sub-divided based on the number of disulfide linkages in their structure.

One line of investigation for the detection of new antimicrobial agents and for the development of more active and stable variants of naturally occurring peptides is the design and chemical synthesis of analogs of natural antimicrobial peptides. The synthesis of hybrid peptides containing portions of the amino acid sequences of two peptides with different antibiotic properties has been a way of optimizing these compounds. Cecropin A, the first known insect antibacterial peptide was found in the hemolymph of *Hyalophora cecropia* pupae [11]. This 37-residue peptide is highly potent and forms a helix-bend-helix motif [12]. Melittin, a 26-amino acid peptide found in the venom of *Apis melifera*, also has strong antibacterial properties but its cytotoxic (hemolytic) properties limit its potential as an antibiotic [13]. The structure of melittin has been investigated under many different conditions, using numerous techniques [14–17] and is composed of two α-helices connected by a hinge. In an attempt to find short antimicrobial peptides with improved activity, a number of hybrid peptides between cecropin A and melittin were synthesized [18–20]. A pentadecapeptide with 1–7 residues (the basic *N*-terminus) of cecropin A and 2–9 residues (the hydrophobic *N*-terminus) of melittin [(CA (1–7) MEL(2–9)] has demonstrated good antibiotic and antimalarial activity [21]. CD studies reveal that this peptide adopts α-helical conformation in 16% hexafluoroisopropanol (HFIP) [22]. Retro and retroenantio analogs of this and other synthetic peptides have been assayed for their antibacterial

*Correspondence to: V. S. Chauhan, International Center for Genetic Engineering and Biotechnology, Aruna Asaf Ali Marg, New Delhi, India; e-mail: virander@icgeb.res.in

Copyright © 2007 European Peptide Society and John Wiley & Sons, Ltd.

WILEY InterScience® DISCOVER SOMETHING GREAT

Table 1 Summary of experimental restraints used for structure calculation of CAMEL peptides and analysis of the family of structures obtained by simulated annealing

Parameter	Peptide			
	CAMEL0	CAMELΔF1	CAMELΔF2	CAMELΔF3
Distance restraints				
All	44	77	97	95
Intraresidue	26	46	43	45
Interresidue	18	31	54	50
Sequential	11	28	36	37
Medium range	7	3	18	13
$i, i+2$	7	1	11	7
$i, i+3$	0	2	7	5
$i, i+4$	0	0	0	1
Long range	0	0	0	0
Average number of violations/structure	3.25	6.60	1.90	2.96
RMSDs with average structure backbone atoms (Å)				
Maximum	2.65	3.36	2.59	2.79
Minimum	2.21	2.28	1.95	2.20
Average	2.43	2.70	2.26	2.63

potency [23] and it was concluded that the chirality of the peptide was not a critical feature in deciding the bioactivity of a peptide [24].

In the present work, we describe the synthesis and conformational studies of the cecropin–melittin hybrid peptide CA (1–7) MEL (2–9), and its three α,β-dehydrophenylalanine (ΔPhe) containing analogs in water–trifluoroethanol mixtures. α,β-dehydroamino acids are characterized by a double bond between Cα and Cβ atoms, and are known to act as stereochemical directors of peptide folding [25]. A number of dehydroanalogs of bioactive peptides have been synthesized and analyzed for biological activity [26]. Another advantage of these modifications is the enhanced resistance of the α,β-dehydroamino acid residue to enzymatic degradation [27]. The peptide sequences described here are 1) Lys-Trp-Lys-Leu-Phe-Lys-Lys-Ile-Gly-Ala-Val-Leu-Lys-Val-Leu **(CAMEL0)** 2) Lys-Trp-Lys-Leu-Phe-Lys-Lys-**ΔPhe**-Gly-Ala-Val-Leu-Lys-Val-Leu (**CAMELΔPhe1**) 3) Lys-Trp-Lys-Leu-**ΔPhe**-Lys-Lys-Ile-Gly-Ala-Val-**ΔPhe**-Lys-Val-Leu (**CAMELΔPhe2**) 4) Lys-Trp-Lys-Leu-**ΔPhe**-Lys-Lys-**ΔPhe**-Gly-Ala-Val-**ΔPhe**-Lys-Val-Leu (**CAMELΔPhe3**). Cecropins have a few conserved residues at the *N*-terminus, e.g. Trp at position 2, Lys at positions 3, 6 and 7. The analogs have been designed keeping these residues unchanged. Only hydrophobic residues were replaced by ΔPhe, thus preserving the amphipathicity of the molecules. Since most antibacterial peptides have been found to be helices, it was proposed that introduction of ΔPhe residues would further stabilize the helical conformation and facilitate a structure-function study.

MATERIALS AND METHODS

Synthesis

All the four cecropin–melittin hybrid peptides were synthesized using Fmoc solid phase synthesis procedure on Wang (*p*-alkoxybenzylalcohol) resin. Lysine and tryptophan side chains were protected with the Boc group. ΔPhe amino acid was introduced as a dipeptide block through azlactonization and dehydration of Fmoc-Lys-D,L-βPheSer-OH, Fmoc-Val-D,L-βPheSer-OH and Fmoc-Leu-D,L-βPheSer-OH to yield Fmoc-Lys-ΔPhe-Azl (azlactone), Fmoc-Val-ΔPhe-Azl and Fmoc-Leu-ΔPhe-Azl respectively, using standard procedures described earlier [28].

Fmoc-Lys-ΔPhe-Azl. Yield 85% m.p. 128–130 °C. $R_f{}^1 = 0.79$. ^{1}H NMR (400 MHz, $CDCl_3$) δ (ppm): 8.08 (t, 1H, ε-NH Lys), 7.8–7.24 (m, 13H, ar-H (Fmoc) + ar-H (ΔPhe)), 7.10 (s, 1H, C$^\beta$H ΔPhe), 5.55 (d, 1H, NH Lys), 4.8–4.4 [m, 3H, CH-CH_2 (Fmoc)], 4.25 (m, 1H, C$^\alpha$H Lys), 3.14 (br, 2H, Lys ε), 1.54–1.42 (m, 6H, Lys C$^\beta$H, Lys C$^\delta$H, Lys C$^\gamma$H).

Fmoc-Leu-ΔPhe-Azl. Yield 67%. m.p.164–166 °C. $R_f{}^1 = 0.82$. ^{1}H NMR (400 MHz, $CDCl_3$) δ (ppm): 8.1–7.26 (m, 13H, ar-H (Fmoc) + ar-H (ΔPhe)), 7.22 (s, 1H, C$^\beta$H ΔPhe), 5.34 (d, 1H, NH Leu), 5.23 (d, 2H, CH_2 Fmoc), 4.51 (m, 1H,CH Fmoc), 4.43 (m, 1H, C$^\alpha$H Leu), 1.66 (m, 2H, C$^\beta H_2$Leu), 1.54 (m, 1H Leu C$^\gamma$H), 0.86–0.99 (m, 6H, 2 x C$^\delta H_3$ Leu).

Fmoc-Val-ΔPhe-Azl. Yield 54%. m.p. 184–186 °C. $R_f{}^1 = 0.73$. ^{1}H NMR (400 MHz, $CDCl_3$) δ (ppm): 8.1–7.21 (m, 13H, ar-H (Fmoc) + ar-H (ΔPhe)), 7.22 (s, 1H, C$^\beta$H ΔPhe), 5.38 (d, 1H, NH Val), 4.50–4.40 (m, 3H, CH-CH_2 Fmoc), 4.25 (m, C$^\alpha$H Val), 2.26 (m, 1H, C$^\beta$H Val), 0.88–1.04 (m, 6H, 2 x C$^\delta H_3$ Leu).

Deprotection and cleavage from the resin were carried out using a mixture of TFA, water and 1,2-ethanedithiol (95 : 2.5 : 2.5 v/v) for two hours at room temperature and the peptides were precipitated in ether. Yield of the final

Copyright © 2007 European Peptide Society and John Wiley & Sons, Ltd.

DOI: 10.1002/psc

peptides: CAMEL0: 84%; CAMEL ΔPhe1: 88%; CAMELΔPhe2: 89%, CAMELΔPhe3: 70%. The crude peptides were purified on reverse phase HPLC using water-acetonitrile gradient on Waters Deltapak C18 (19 mm × 300 mm) column. The molecular mass of the peptides, determined by ES-MS, were (a) CAMEL0: 1770.34 (calculated 1771.6), CAMELΔPhe1: 1802.9 (calculated 1804.6), CAMELΔPhe2 1801.2 (calculated 1803.6), CAMELΔPhe3 1835.7 (calculated 1836.6).

Antibacterial and Erythrocyte Lysis Assays

The antibacterial activity was tested using the microtitre broth dilution method [29], for *Escherichia coli* ATCC 11 303 and *Staphylococcus aureus* ATCC 259 230, as modified by Hancock. 1mM stock solutions of all the four peptides were prepared in 0.01% acetic acid and 0.2% BSA. Serial dilutions of each peptide were made in MHB (Mueller Hinton Broth) in 96-well microtiter plates. 11 μl peptide (concentration varying from 4.68 μM to 100 μM) was added to each well. Each well was inoculated with 99 μl of 10^4–10^5 CFU of the test organism per ml. The absorbance was recorded at 650 nm after incubating the plates for 18 h at 37 °C. The cultures were then plated on MHA (Meuller Hinton Agar) and incubated overnight to determine a viable count. The minimum inhibitory concentration (MIC) was taken as the lowest concentration at which cell death starts.

Freshly collected mouse blood was washed thrice with PBS (35 mM phosphate buffer, 0.15 M NaCl, pH 7.0) and the erythrocytes were pelleted out by centrifugation. They were resuspended in PBS (0.4% v/v) for the assay. 100 μl of the suspended erythrocytes and the same volume of peptides (final peptide concentration ranged from 3.12 μM to 100 μM), were added to each well of the microtitre plate. The plates were incubated with rocking at 37 °C, and the concentration required for lysis was determined after 1 h. Zero and 100% hemolysis were determined in PBS and Triton X-100 respectively. Release of hemoglobin was measured by absorbance at 405 nm. Percent hemolysis was calculated by the formula, % hemolysis = [(A_{405} in peptide solution) − (A_{405} in PBS)]/[A_{405} in Triton X-100) − (A_{405} in PBS)].

Circular Dichroism Spectroscopy

Raw data were recorded in water/trifluoroethanol solvent mixtures. The aqueous solutions simulate the extracellular matrix, while solutions containing high amounts of trifluroethanol simulate a membrane-like environment. CD spectra in 100% water (0% TFE) and in TFE with varying concentration from 10 to 100% in steps of 10% were recorded. For each run, four scans from 350 to 195 nm were averaged.

NMR Studies and Structure Generation

The peptides were dissolved in H_2O:D_2O (9:1), H_2O:TFE-d_3 (1:1) and H_2O:TFE-d_3 (1:9) to yield a concentration of 2 mM at pH 5.0 and the spectra were acquired at 298 K using a Varian 600 MHz NMR spectrometer. All chemical shifts were referenced to the methyl resonance of 2,2-dimethyl-2-silapentane-1-sulfonate (DSS, 0 ppm). States-Haberkorn method was used for quadrature detection. Sequences employing water gate method were used for solvent suppression. TOCSY [30] and NOESY [31] experiments were carried out with mixing times of 75 and 300 ms, respectively for identification of spin systems and for sequential assignments. NOESY experiments at 150, 250 and 400 ms were also recorded for obtaining buildup curves at 50% TFE concentration. DQF COSY [32] spectra were acquired with 500 t_1 increments, 32 scans and 2 K data points in the t_2 dimension. The spectra were processed using the software Felix v. 97.2. For 2D experiments, the F2 and F1 dimensions were zero-filled to 1K data points and $\pi/2$ phase shifted sine squared window function was applied along both the dimensions.

To estimate distances from the NOESY spectra for calculation of the secondary structure, the peaks were classified as strong, medium and weak, corresponding to the distance ranges of 1.8–2.7, 2.7–3.5 and 3.5–5.0 Å. Well resolved NOESY peaks between geminal protons of the side chains of Leu or Ile were used as reference peaks since the distance (1.75 Å) between geminal protons is independent of conformation. Pseudoatom corrections were used. The total number of restraints calculated for CAMEL0, CAMELΔPhe1, CAMELΔPhe2 and CAMELΔPhe3 were 44, 77, 97 and 95 respectively (Table 1). All molecules were minimized before being subjected to simulated annealing (SA) calculations with the DISCOVER (Accelrys Inc.) program using the cvff forcefield. The SA started with an extended conformation of the peptide backbone. The molecules were then heated to 1000 K and slowly cooled in steps of 100–300 K. The dynamics was carried out for 40 ps and then minimized using 2000 steps of steepest gradients, 3000 steps of conjugate gradients and 200 steps of va09a. A total of 50 structures were generated for each peptide.

RESULTS AND DISCUSSION

Conformational Analysis by Circular Dichroism Spectroscopy

A number of CD studies characterizing the shape of the CD spectrum to the conformation of ΔPhe containing peptides have been carried out in the near UV region [33]. Almost all of these studies have been carried out in apolar solvents such as chloroform, dimethylsulfoxide, methanol, etc. Very few reports of the CD spectra of water-soluble ΔPhe containing peptides are available in literature [34]. In the following text, we describe the CD results for the four peptides in water-TFE mixtures.

Figure 1 shows the CD spectra of all four peptides with increasing concentration of trifluoroethanol. In 100% aqueous solution, the peptides are largely random. With increasing TFE concentration, the conformation of peptides stabilize. For CAMELΔPhe0, the isodichroic point at ~203 nm indicates that the peptide is visiting two conformational states; coil-helix transition taking place on changing the solvent from water to TFE (Figure 1(a)). At 80% TFE, two minima at 207 nm and 225 nm and a positive band at 195 nm are observed, which are characteristic of a α-helix [35]. In case of CAMELΔPhe1, a negative maximum at ~203 nm along with a shoulder at ~230 nm at

Copyright © 2007 European Peptide Society and John Wiley & Sons, Ltd.

DOI: 10.1002/psc

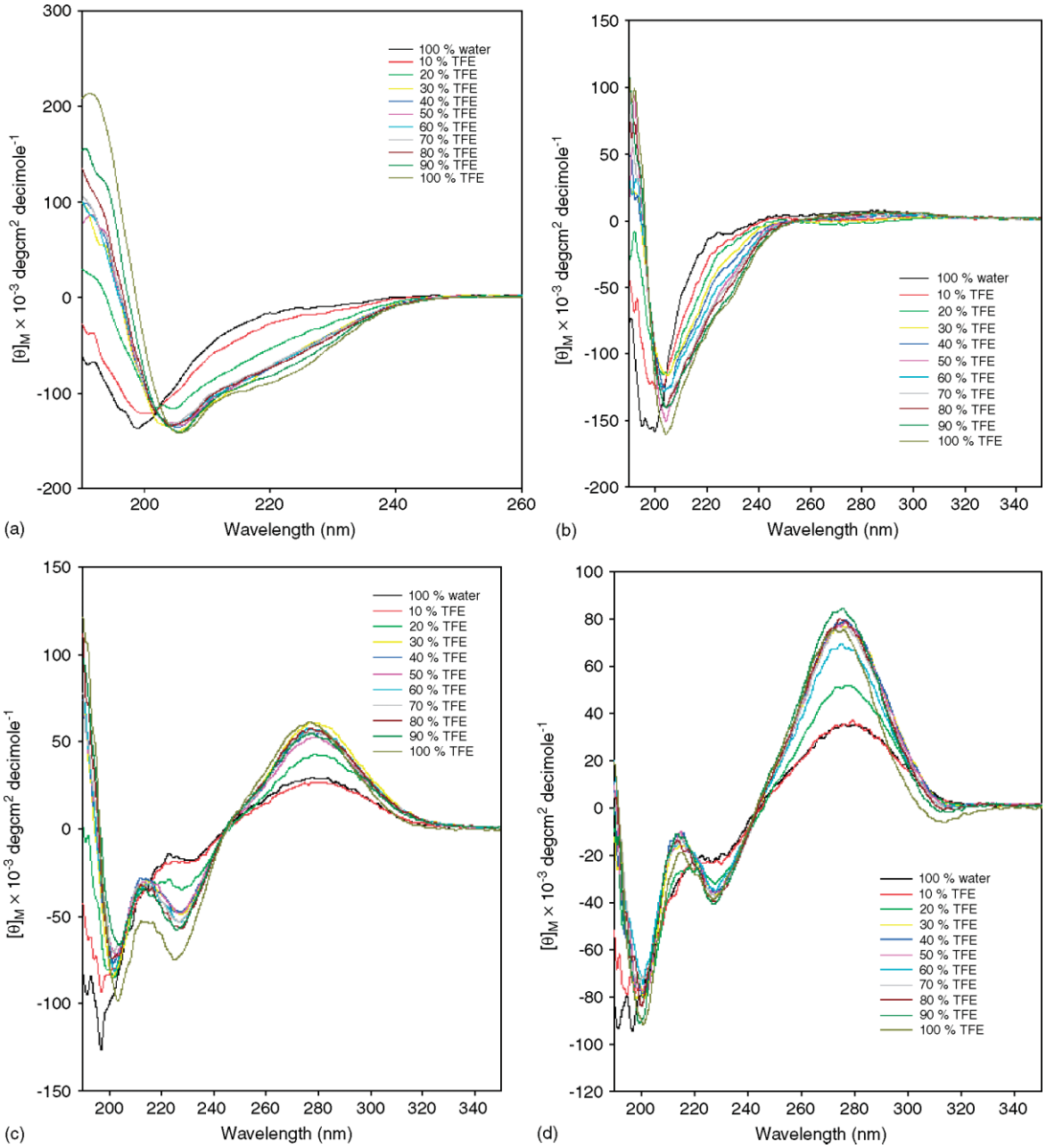

Figure 1 CD spectra of the peptides (a) CAMEL0 (b) CAMELΔF1 (c) CAMELΔF2 (d) CAMELΔF3, depicting water-TFE titrations.

higher TFE concentrations corresponds to a type U CD spectrum [36] characteristic of aperiodic or unordered conformation (Figure 1(b)). Surprisingly, no band was observed at ~280 nm, which is characteristic of a ΔPhe amino acid [33]. This further suggests that the peptide is flexible and ΔPhe is not involved in forming any rigid structure.

Though largely aperiodic at lower TFE concentration, CAMELΔPhe2 assumes stabilization in secondary structure at higher TFE ratios (Figure 1(c)). A positive signal at 195 nm is accompanied by two negative bands at ~205 nm and ~228 nm respectively. This pattern can be attributed to type C spectrum (quite similar to α-helix) which implies the presence of type I, III and II′β-turns [37,38]. It has also been proposed earlier that a class C spectrum may be related to 3_{10}-helix or mixtures of α-helix and random conformers [39]. The second negative band at ~228 nm is separated from the minimum at ~205 nm by a relative maximum at ~217 nm. Tryptophan residues are expected to contribute to CD spectra in the far-UV region that is associated with the peptide bond [40]. This conclusion is based on the calculations discussed by Woody [41] and studies of gramicidin [42] and other tryptophan containing membrane-binding peptides [43]. The negative peak at ~228 nm, observed in the CD spectrum of CAMELΔPhe2 peptide, can therefore be attributed to the tryptophan side chain.

Copyright © 2007 European Peptide Society and John Wiley & Sons, Ltd.

DOI: 10.1002/psc

It has been reported that the coupling of a negative peak at 227 nm with the positive peak at 217 nm is characteristic of the stacking of aromatic rings [40,44]. In the present context however, this couplet assumes importance in light of the possible Trp-ΔPhe stacking interactions. This suggests an arrangement in which Trp and ΔPhe come together in some kind of turn conformation. With increasing TFE concentration, an increase in the 228 nm band is observed at the expense of the 205 nm band which indicates further stabilization of this interaction. The positive peak at ~280 nm arises from the chirally perturbed ΔPhe chromophore [45].

The CD spectrum for CAMELΔPhe3 (Figure 1(d)) constitutes a weakly positive band at ~195 nm, a strong negative signal at ~200 nm and a weaker one at ~227 nm, separated by a relative maximum at 215 nm. This can be termed as *transitional spectra* with curve shapes between type C and type U spectra. Such spectra are indicative of conformational equilibrium between β-turns and an aperiodic peptide chain [36]. The coupling of negative band at 227 nm with the positive one at 215 nm could be attributed to the stacking interactions between Trp^2, ΔPhe^5 and/or ΔPhe^8. An intense peak at ~275 nm arises from the chirally perturbed ΔPhe chromophores. Simultaneously, the presence of another negative band at 227 nm may well be diagnostic for a ΔPhe residue included in a type III β-bend [33].

Structural Analysis by ^{1}H NMR

The NMR structures for all the peptides were solved at solvent composition H_2O : TFE-d_3, 1 : 1. Identification of spin systems was carried out using TOCSY. NOESY spectra were used to obtain interresidue connectivities and to distinguish equivalent spin systems. The ΔPhe NHs were easily assigned as they resonate as singlets, shifted maximally downfield. Singly occurring amino acids were assigned to Trp^2, Gly^9 and Ala^{10}, except Ile, which has a pattern similar to Leu. Using these uniquely assigned residues as starting points, together with the sequential NOE connectivities, the sequence specific resonance assignments of all the four peptides could be completed. Figure 2 illustrates the identification of 12 spin systems for CAMELΔPhe2 peptide.

Spatial proximity through NOE and structure determination. The CAMEL0 peptide with no ΔPhe residue, shows a few strong and medium-range scattered NOEs of the type d_{NN} and $d_{\alpha N}$ in 50% TFE-water mixture (Figure 3(a)). A few medium-range NOEs such as $d_{\alpha N}(i, i+2)$ and $d_{\alpha N}(i, i+3)$ were also observed due to the presence of a significant population of $\beta(i)\alpha(i+1)$ and $\alpha(i)\alpha(i+1)$ conformers [46,47]. A total of 44 restraints were used for the determination of structures by SA. Such a small number of restraints is also an

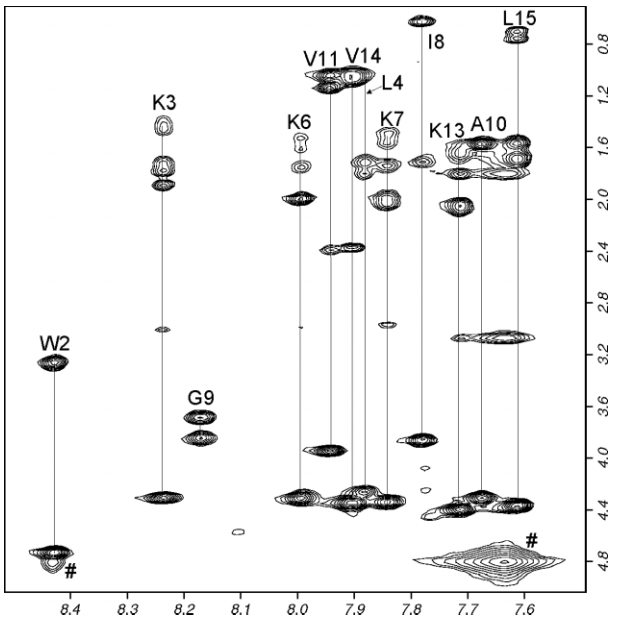

Figure 2 C^{α}H-NH region of the TOCSY spectrum for CAMELΔF2 peptide showing spin system for each residue. ΔPhe^5 and ΔPhe^{12} resonate further downfield and are hence, not visible. # represents artifacts in the NMR spectrum.

indication of the random nature of the peptide. For the CAMELΔPhe1 peptide, only sequential NOEs, d_{NN}, $d_{\alpha N}$ and $d_{\beta N}$ were observed (Figure 3(b)). Moderate-intensity d_{NN} and strong $d_{\alpha N}$ peaks, especially in the *N*-terminal half of the peptide indicate an extended conformation (Figure 4(b)). A total of 77 restraints were used for structure calculation. CAMELΔPhe2 shows a number of sequential and medium-range NOEs indicating the stabilization of a secondary structure (Figures 3(c) and 4(c)). Continuous strong d_{NN} peaks were seen almost through the entire length of the peptide from Leu^4 to Leu^{15} indicating a helical conformation. Medium-range $d_{\alpha N}(i, i+3)$ and $d_{\alpha N}(i, i+2)$ peaks suggest the presence of a 3_{10}-helix in the *C*-terminal half of the peptide from Lys^7 to Val^{14} (Figure 4(c)) [48]. Strong d_{NN} cross-peaks ΔF5/K6 and K6/K7 and a medium-intensity $d_{\beta N}$ between ΔF5/K6 suggests the presence of a type I β-turn involving the segment, Leu^4-ΔPhe^5-Lys^6-Lys^7. For quantitative estimation of NOEs, a total of 97 restraints including 43 intra-residue and 54 inter-residual restraints were calculated. A total of 50 structures were generated using the SA protocol. The average structure is shown in Figure 5(a). The structure represents a type I β-turn from Leu^4-Lys^7, followed by a helix at the *C*-terminus. The turn was stabilized by one $i \leftarrow i+3$ hydrogen bond between C=OLeu^4 and NHLys^7. A similar hydrogen bond was also observed between C=OLys^7 and NHAla^{10}, the first turn of a 3_{10}-helix. Another hydrogen bond of the type $i \leftarrow i+4$ between C=OAla^{10} and NHVal^{14} was satisfied in most of the structures calculated, suggesting a $1 \leftarrow 5$ turn. CAMELΔPhe3 peptide shows continuous

Copyright © 2007 European Peptide Society and John Wiley & Sons, Ltd.

DOI: 10.1002/psc

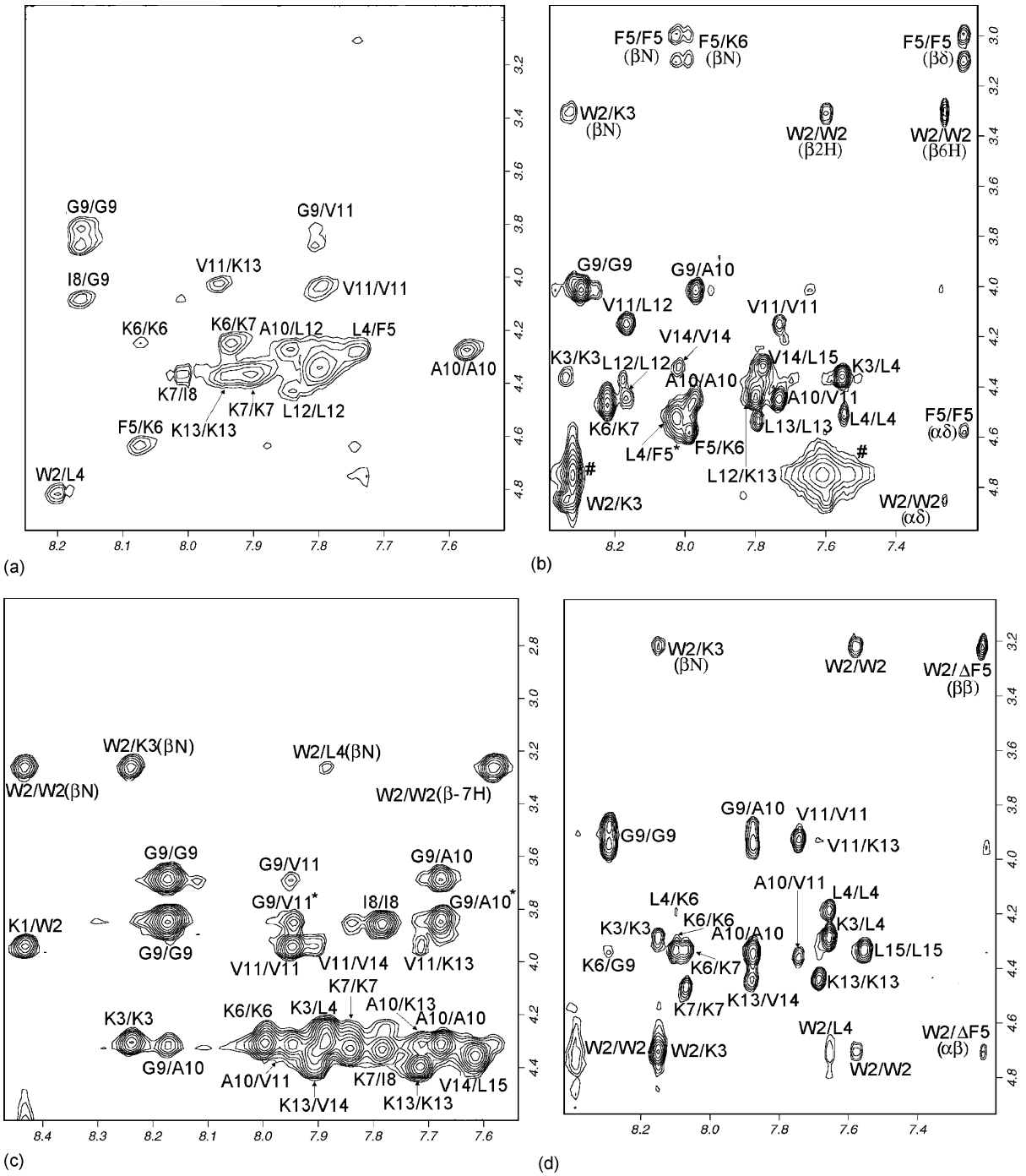

Figure 3 Fingerprint region of the NOESY spectra (300 ms) for peptides (a) CAMEL0 (b) CAMELΔF1 (c) CAMELΔF2 (d) CAMELΔF3, showing self, sequential and medium range peaks. A few sidechain–backbone as well as sidechain–sidechain NOEs are also labeled.

d_{NN} NOE cross-peaks from Lys^7 to Leu^{15} (Figure 4(d)). Medium-intensity NOE peaks of the type $d_{\alpha N}(i, i+2)$ and $d_{\alpha N}(i, i+3)$ force residues V^{11}, ΔF^{12}, K^{13} and V^{14} to fold into a β-turn (Figure 3(d)). A strong NOE of the $d_{\alpha N}$ type between K3/L4 and medium-intensity $d_{\alpha N}(i, i+2)$ peaks suggest a type II β-turn between W^2, K^3, L^4 and ΔF^5. A medium-intensity $d_{\beta N}(i, i+4)$ NOE between ΔF5/G9 brings ΔPhe^5 and Gly^9 close in space. Out of a total of 95 restraints calculated, 45 were intra and 50 were interresidue peaks. Figure 5(b) shows the average structure calculated for the peptide CAMELΔPhe3. In this case, only a single hydrogen bond of the type $i \leftarrow i+3$ was observed between C=O Val^{11} and NH Val^{14} in most of the structures calculated by SA.

For flexible peptides in solution, the coupling constants represent an ensemble average and are of less value than other parameters in distinguishing between various types of secondary structures. This

Copyright © 2007 European Peptide Society and John Wiley & Sons, Ltd.

DOI: 10.1002/psc

is consistent with the observed $^3J_{N\alpha}$ coupling constants (7–9 Hz), which approach the values for a β-strand [49]. A database of 85 high-resolution protein crystal structures has been used to predict $^3J_{N\alpha}$ values in coil regions and have been correlated with experimental values. These values range from 5.8 to 7.7 Hz [50]. All four of the peptides discussed show $^3J_{N\alpha}$ values in the range 7–8.5 Hz, characteristic of population-weighted random coil models. The exact values are given in Figure 4. A number of $^3J_{N\alpha}$ values could not be reported due to narrow dispersion of $C^{\alpha}H$ values and therefore overlapping of peaks, especially the CAMEL0 peptide.

Ratio of NOE intensities. A recent description of the random coil conformation from a statistical analysis of ϕ,ψ distributions in the coil regions of protein high-resolution X-ray structures has led to a population-weighted description of backbone torsion angles from which both short and medium range NOEs can be calculated [46,47]. This population-weighted random coil model provides a useful reference for identifying deviations indicative of local structure formation in peptides, protein fragments and denatured states of proteins. In this model, all sequential $C^{\alpha}H$–NH and NH–NH NOEs (abbreviated as $\alpha N(i, i+1)$ and $NN(i, i+1)$, respectively) are observed, reflecting significant populations of both α and β conformers for each residue in the random coil. Two ratios, namely, $\alpha N(i, i+1)/NN(i, i+1)$ and $\alpha N(i, i+1)/\alpha N(i, i)$ have been extensively studied. We have calculated these ratios for our peptides to detect local structure formation.

αN(i, i + 1)/NN(i, i + 1). CAMEL0 peptide shows very few NOEs. The ratio could be obtained for only three residues with an average value of 1.8, which corresponds to a random structure. CAMELΔPhe1 shows an average value of 4.0 which is a little higher than that observed for random coil, but not large enough to be characterized as a β-sheet. In case of the CAMELΔPhe2 peptide, these ratios from residue I8 -L15 are close to 0.5, indicating helical conformation. CAMELΔPhe3 depicts ratios closer to the value of 1.0, suggesting β-turns [51].

αN(i, i + 1)/αN(i, i). This ratio in CAMEL0 and CAMEL-ΔPhe1 peptides shows average values of 1.63 and 2.15 respectively, close to that reported for the population-weighted random coil model which is 2.3. CAMELΔPhe2 with ratio of 0.5, indicates a helical conformation with $\alpha N(i, i)$ peaks stronger than $\alpha N(i, i+1)$. The ratio for CAMELΔPhe3 shows values ranging from 0.5–1.0, suggesting β-turns [51].

Antibacterial and Hemolytic Activity

A representative bacterium from each type, gram-positive (*S. aureus* ATCC 259 230) and gram-negative (*E. coli* ATCC 11 303), were chosen to perform antibacterial activity. Colony forming units were counted at all concentrations plated for both bacterial strains. MIC is taken as the lowest concentration of the peptide at which cell death starts and is reported in Table 2. Figure 6 shows the plot of percentage increase in antibacterial activity of CAMELΔPhe1, CAMELΔPhe2 and CAMELΔPhe3 with respect to the wild type CAMEL0 peptide, as calculated from their respective MIC values. All three ΔPhe containing analogs show increased activity against both the strains (except CAMELΔPhe3, which shows no increase in activity as compared to the wild type peptide for *S. aureus* strain). CAMELΔPhe2 peptide is maximally potent against both the bacterial species. CAMELΔPhe1 is more active against the gram-negative strain, *E. coli* ATCC 11 303.

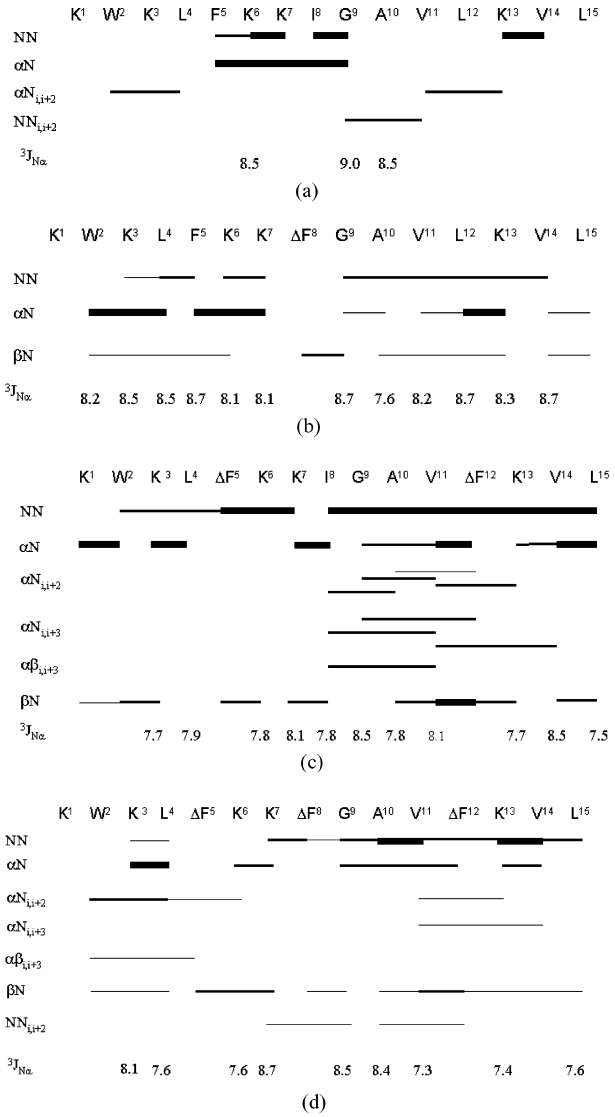

Figure 4 Summary of NOE peaks for (a) CAMEL0 (b) CAMELΔF1 (c) CAMELΔF2 (d) CAMELΔF3. The thick, medium-intensity and thin bars represent strong, medium and weak NOEs respectively.

Copyright © 2007 European Peptide Society and John Wiley & Sons, Ltd.

DOI: 10.1002/psc

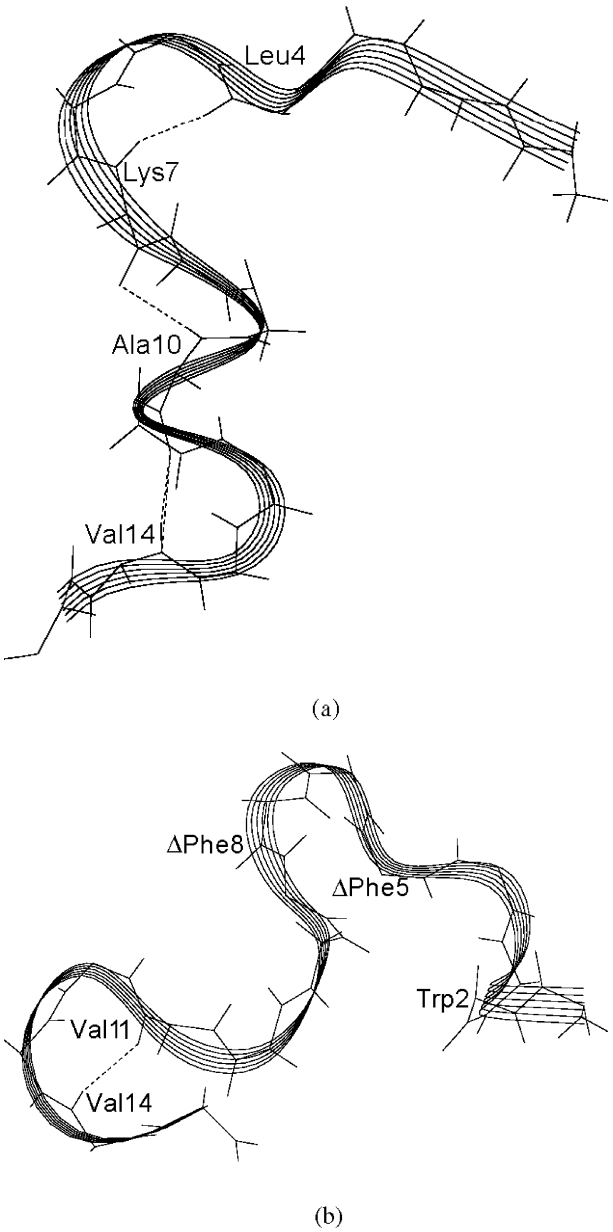

Figure 5 A ribbon diagram of the average conformation of (a) CAMELΔF2 (b) CAMELΔF3 peptide. Hydrogen bonds satisfying the Baker & Hubbard criteria in most of the calculated structures are shown as dotted lines.

Table 2 MIC of the four CAMEL peptides against the two test organisms

Peptide	*S. aureus* 259 230 (μM)	*E. coli* 11 303 (μM)
CAMEL0	50	50
CAMELΔPhe1	37.5	12.5
CAMELΔPhe2	18.75	12.5
CAMELΔPhe3	50	37.5

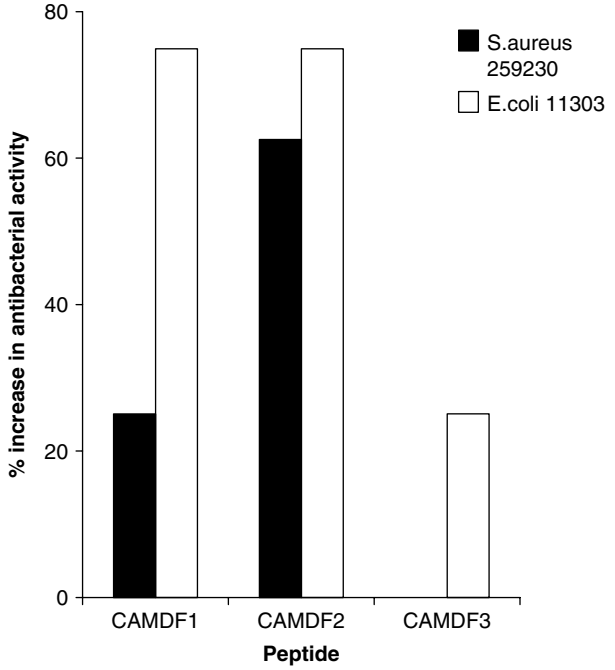

Figure 6 Plot of percentage increase in antibacterial activity (calculated from MIC values) shown by the three analogs namely, CAMELΔF1, CAMELΔF2 and CAMELΔF3, relative to the wild type CAMEL0 peptide.

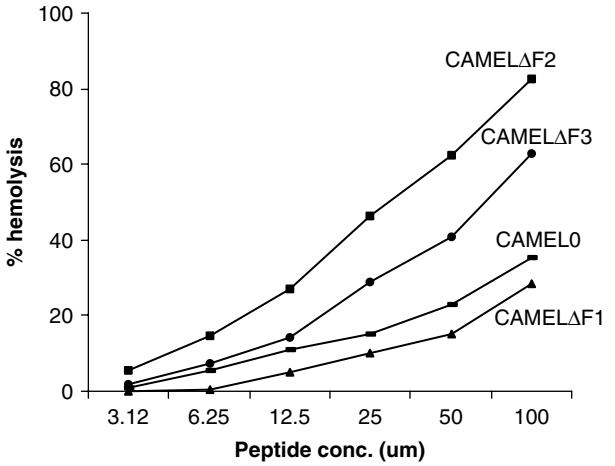

Figure 7 Hemolytic activity of the CAMEL peptides. % hemolysis is plotted against peptide concentration.

CAMELΔPhe1 with a single ΔPhe at the center shows minimal hemolysis. CAMELΔPhe2 and CAMELΔPhe3 are quite hemolytic with the former showing maximum hemolysis (Figure 7).

CONCLUSION

The cecropin–melittin hybrid peptide CAMEL0 and three of its analogs CAMELΔPhe1, CAMELΔPhe2 and CAMELΔPhe3 were synthesized by solid-phase method and their conformation determined by CD and NMR.

Copyright © 2007 European Peptide Society and John Wiley & Sons, Ltd.

DOI: 10.1002/psc

Given the known propensity of ΔPhe to stabilize helical structures, introduction of this residue at various positions along the sequence of CAMEL0 was expected to stabilize a helical conformation. This effect has been shown by the CAMELΔPhe2 peptide containing two ΔPhes at positions 5 and 12, respectively, where a helical conformation is stabilized at the *C*-terminus. A single ΔPhe in the middle of the sequence in CAMELΔPhe1, does not appear sufficient to stabilize a helical structure in the peptide. Introduction of three ΔPhe residues stabilizes isolated turns in the peptide CAMELΔPhe3, but not a helix. This result was somewhat surprising, since we had expected a higher degree of helicity of this peptide with three ΔPhe residues. Circular dichroism studies for CAMELΔPhe2 and CAMELΔPhe3 suggest the presence of Trp-ΔPhe interactions. CAMELΔPhe2 peptide shows the best antibacterial activity, though hemolytic at the same time. Although a number of hydrophobic peptides containing ΔPhe are well known to stabilize helices, the conformational preference of ΔPhe in the presence of polar amino acids is less studied. Further studies are warranted to explore the conformational preferences of ΔPhe in water-soluble peptides in order to derive a structure–activity relationship.

Acknowledgements

Financial support from the Department of Science and Technology (DST SP/SO/D35/96), India, is acknowledged. We thank the NMR facility at TIFR, Mumbai, India, for NMR data acquisition.

REFERENCES

1. Boman HG, Hultmark D. Cell-free immunity in insects. *Annu. Rev. Microbiol.* 1987; **41**: 103–126.
2. Boman HG. Peptide antibiotics and their role in innate immunity. *Annu. Rev. Immunol.* 1995; **13**: 61–92.
3. McPhee JB, Hancock REW. Function and therapeutic potential of host defence peptides. *J. Pept. Sci.* 2005; **11**: 677–687.
4. Otvos L. Antibacterial peptides and proteins with multiple cellular targets. *J. Pept. Sci.* 2005; **11**: 697–706.
5. Zasloff M. Antimicrobial peptides of multicellular organisms. *Nature* 2002; **415**: 389–395.
6. Hancock REW, Scott MG. The role of antimicrobial peptides in animal defenses. *Proc. Natl. Acad. Sci. U.S.A.* 2000; **97**: 8856–8861.
7. Hancock REW, Chapple DS. Peptide antibiotics. *Antimicrob. Agents Chemother.* 1999; **43**: 1317–1323.
8. Ganz T, Lehrer RI. Antibiotic peptides from higher eukaryotes: biology and applications. *Mol. Med. Today* 1999; **5**: 292–297.
9. Epand RM, Vogel HJ. Diversity of antimicrobial peptides and their mechanisms of action. *Biochim. Biophys. Acta* 1999; **1462**: 11–28.
10. Hwang PM, Vogel HJ. Structure-function relationships of antimicrobial peptides. *Biochem. Cell Biol.* 1998; **76**: 235–246.
11. Hultmark D, Steiner H, Rasmusson T, Boman HG. Insect immunity: purification and properties of three inducible bactericidal proteins from hemolymph of immunized pupae of Hyalophora cecropia. *Eur. J. Biochem.* 1980; **106**: 7–16.
12. Holak TA, Engstrom A, Kraulis PJ, Lindeberg G, Bennich H, Jones TA, Gronenborn AM, Clore GM. The solution conformation of the antibacterial peptide cecropin A: a nuclear magnetic resonance and dynamical simulated annealing study. *Biochemistry* 1988; **27**: 7620–7629.
13. Habermann E, Jentsch J. Sequence analysis of melittin from tryptic and peptic degradation products. *Hoppe-Seyler's Z. Physiol. Chem.* 1967; **348**: 37–50.
14. Vogel H, Jahnig F. The structure of melittin in membranes. *Biophys. J.* 1986; **50**: 573–582.
15. Terwilliger TC, Eisenberg D. The structure of melittin. I. Structure determination and partial refinement. *J. Biol. Chem.* 1982; **257**: 6010–6015.
16. Brown LR, Wuthrich K. Melittin bound to dodecylphosphocholine micelles. H-NMR assignments and global conformational features. *Biochim. Biophys. Acta* 1981; **647**: 95–111.
17. Bazzo R, Tappin MJ, Pastore A, Harvey TS, Carver JA, Campbell ID. The structure of melittin. A ^{1}H-NMR study in methanol. *Eur. J. Biochem.* 1988; **173**: 139–146.
18. Oh D, Shin SY, Kang JH, Hahm KS, Kim KL, Kim Y. NMR structural characterization of cecropin A (1–8)-magainin 2 (1–12) and cecropin A (1–8)-melittin (1–12) hybrid peptides. *J. Pept. Res.* 1999; **53**: 578–589.
19. Shin SY, Kang JH, Hahm KS. Structure-antibacterial, antitumor and hemolytic activity relationships of cecropin A-magainin 2 and cecropin A-melittin hybrid peptides. *J. Pept. Res.* 1999; **53**: 82–90.
20. Vunnam S, Juvvadi P, Rotondi KS, Merrifield RB. Synthesis and study of normal, enantio, retro and retroenantio isomers of cecropin A-melittin hybrids, their end group effects and selective enzyme inactivation. *J. Pept. Res.* 1998; **51**: 38–44.
21. Andreu D, Ubach J, Boman A, Wahlin B, Wade D, Merrifield RB, Boman HG. Shortened cecropin A-melittin hybrids. *FEBS Lett.* 1992; **296**: 190–194.
22. Fernandez I, Ubach J, Reig F, Andreu D, Pons M. Effect of succinylation on the membrane activity and conformation of a short cecropin A-melittin hybrid peptide. *Biopolymers* 1994; **34**: 1251–1258.
23. Merrifield RB, Juvvadi P, Andreu D, Ubach J, Boman A, Boman HG. Retro and retroenantio analogs of cecropin-melittin hybrids. *Proc. Natl. Acad. Sci. U.S.A.* 1995; **92**: 3449–3453.
24. Wade D, Boman A, Wahlin B, Crain CM, Andreu D, Boman HG, Merrifield RB. All D amino acid containing channel-forming antibiotic peptides. *Proc. Natl. Acad. Sci. U.S.A.* 1990; **87**: 4761–4765.
25. Joshi RM, Chauhan VS. Synthesis of peptides and peptidomimetics. *Houben-Weyl* 2003; **E22**: 635–662.
26. Mathur P, Ramakumar S, Chauhan VS. Peptide design using α,β-dehydroamino acids: From β-turns to helical hairpins. *Biopolymers* 2004; **76**: 150–161.
27. English ML, Stammer CH. The enzyme stability of dehydropeptides. *Biochem. Biophys. Res. Commun.* 1978; **83**: 1464–1467.
28. Ramagopal UA, Ramakumar S, Sahal D, Chauhan VS. De novo design and characterization of an apolar helical peptide at atomic resolution: compaction mediated by weak interactions. *Proc. Natl. Acad. Sci. U.S.A.* 2001; **98**: 870–874.
29. Amsterdam D. Susceptibility testing of Antimicrobials in liquid media. In *Antibiotics in Laboratory Medicine*, 4th edn, Lorian V (ed.). Williams and Wilkins: Baltimore, MD, 1996; 52–111.
30. Braunschweiler L, Ernst RR. Coherence transfer by isotropic mixing: application to proton correlation spectroscopy. *J. Magn. Reson.* 1983; **53**: 521–528.
31. Jeener J, Meier BH, Bachmann P, Ernst RR. Investigation of exchange processes by two-dimensional NMR spectroscopy. *J. Chem. Phys.* 1979; **71**: 4546–4553.
32. Muller N, Ernst RR, Wuthrich K. Multiple-quantum filtered two-dimensional correlated NMR spectroscopy of proteins. *J. Am. Chem. Soc.* 1986; **108**: 6482–6492.
33. Pieroni O, Fissi A, Jain RM, Chauhan VS. Solution structure of dehydropeptides: A CD investigation. *Biopolymers* 1996; **38**: 97–108.

Copyright © 2007 European Peptide Society and John Wiley & Sons, Ltd.

34. Chetal P, Chauhan VS, Sahal D. A meccano set approach of joining trpzip a water soluble beta-hairpin peptide with a didehydrophenylalanine containing hydrophobic helical peptide. *J. Pept. Res.* 2005; **65**: 475–484.
35. Tinoco I, Woody RW, Bradley DF. Absorption and rotation of light helical polymers. Effect of chain length. *J. Chem. Phys.* 1963; **38**: 1317–1325.
36. Hollosi M, Otvos L Jr, Urge L, Kajtar J, Percel A, Lacko I, Vadasz ZS, Fasman GD. Ca^{2+} induced conformational transitions of phosphorylated peptides. *Biopolymers* 1993; **33**: 497–510.
37. Gierasch LM, Deber CM, Madison V, Niu CH, Blout ER. Conformations of $(X\text{-}L\text{-}Pro\text{-}Y)_2$ cyclic hexapeptides. Preferred beta-turn conformers and implications for beta turns in proteins. *Biochemistry* 1981; **20**: 4730–4738.
38. Rose GD, Gierasch LM, Smith JA. Turns in peptide and proteins. *Adv. Protein Chem.* 1985; **37**: 1–109.
39. Perczel A, Hollosi M. In *Circular Dichroism and Conformational Analysis of Biomolecules*, Fasman GD (ed.). Plenum Press: New York, 1996; 285–380.
40. Arnold GE, Day LA, Dunker AK. Tryptophan contributions to the unusual circular dichroism of fd bacteriophage. *Biochemistry* 1992; **31**: 7948–7956.
41. Woody RW. Contributions of tryptophan side chains to the far-ultraviolet circular dichroism of proteins. *Eur. Biophys. J.* 1994; **23**: 253–262.
42. Woolley GA, Dunn A, Wallace BA. Gramicidin-lipid interactions induce specific tryptophan side-chain conformations. *Biochem. Soc. Trans.* 1992; **20**: 864–867.
43. Wimley WC, Hristova K, Ladokhin AS, Silvestro L, Axelsen PH, White SH. Folding of beta-sheet membrane proteins: a hydrophobic hexapeptide model. *J. Mol. Biol.* 1998; **277**: 1091–1110.
44. Grishina IB, Woody RW. Contributions of tryptophan side chains to the circular dichroism of globular proteins: exciton couplets and coupled oscillators. *Faraday Discuss.* 1994; **99**: 245–262.
45. Jain RM, Chauhan VS. Conformational characteristics of peptides containing α,β-dehydroamino acid residues. *Biopolymers (Pept. Sci.)* 1996; **40**: 105–119.
46. Fiebig KM, Schwalbe H, Buck M, Smith LJ, Dobson CM. Toward a description of the conformations of denatured states of proteins. Comparison of a random coil model with NMR measurements. *J. Phys. Chem.* 1996; **100**: 2661–2666.
47. Smith LJ, Fiebig KM, Schwalbe H, Dobson CM. The concept of a random coil. Residual structure in peptides and denatured proteins. *Fold Des.* 1996; **1**: R95–106.
48. Wuthrich K. *NMR of Proteins and Nucleic Acids*. John Wiley and Sons: New York, 1986.
49. Dyson HJ, Rance M, Houghten RA, Wright PE, Lerner RA. Folding of immunogenic peptide fragments of proteins in water solution. II. The nascent helix. *J. Mol. Biol.* 1988; **201**: 201–217.
50. Smith LJ, Fiebig KM, Schwalbe H, MacArthur MW, Thornton JM, Dobson CM. Analysis of main chain torsion angles in proteins: Prediction of NMR coupling constants for native and random coil conformations. *J. Mol. Biol.* 1996; **255**: 494–506.
51. Sharman GJ, Searle MS. Cooperative interaction between the three strands of a designed antiparallel β-sheet. *J. Am. Chem. Soc.* 1998; **120**: 5291–5300.

Copyright © 2007 European Peptide Society and John Wiley & Sons, Ltd.

DOI: 10.1002/psc